Food Chemistry: X 36 (2026) 103839

Contents lists available at ScienceDirect

Food Chemistry: X

journal homepage: www.sciencedirect.com/journal/food-chemistry-x

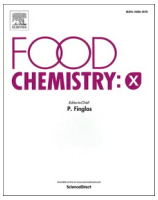

Integrated analysis of proteomics and metabolomics revealed mechanisms underlying age-related changes in pigeon breast muscle

Ying Wang [1], Dongzhi Miao [1], Jing Chen, Haodong Zhang, Wanqing Li, Haiming Yang [*], Zhiyue Wang

College of Animal Science and Technology, Yangzhou University, Yangzhou, Jiangsu Province 225009, China

ARTICLE INFO

Keywords:
Proteomics
Metabonomics
Pigeon
Breast
Meat quality

ABSTRACT

This study conducted a comprehensive comparison of the metabolomic and proteomic profiles of pigeon breast muscles from 12-month-old (M12) and 28-day-old (D28) birds to investigate the influence of age on meat quality. The M12 samples showed lower L*, a*, and b* values but higher ΔpH, shear force, cooking loss, hardness, cohesiveness, and gumminess compared to the D28 samples. Metabolomic analysis identified five down-regulated metabolites, L-histidine (fold change, FC = 0.216), L-arginine (FC = 0.560), 4-hydroxyproline (FC = 0.149), D-sedoheptulose 7-phosphate (FC = 0.465), and L-glutamic acid 5-phosphate (FC = 0.120), that were primarily involved in amino acid and related metabolic pathways, differentiating the two groups. Proteomic profiling revealed a reduced abundance of several proteins, importantly A306_00011918, A306_00011919, ENPP1, TKT, and ALDH18A1, which are involved in amino acid biosynthesis in M12. Integrative analysis of metabolomic and proteomic data highlighted amino acid biosynthesis, mediated by specific metabolites and proteins, as the major differentiating pathway between M12 and D28. In conclusion, these findings provide mechanistic insights into the molecular basis underlying age-dependent variations in pigeon meat quality, offering valuable guidance for poultry producers in determining the optimal slaughter age to achieve desirable meat characteristics.

1. Introduction

Pigeon meat, valued for its high nutritional content, is widely consumed across various culinary traditions and global markets (Chang et al., 2023). Different pigeon ages are preferred for specific culinary and commercial purposes. For instance, 28-day-old pigeons are commonly used in large-scale meat production due to their superior economic efficiency (Yang et al., 2025). In comparison, older pigeons are traditionally utilized in dishes such as Cantonese-style pigeon soup in Chinese cuisine (Jiang et al., 2022). Gao et al. (2016) reported that pigeon body weight stabilizes after 28 days of age, coinciding with a decline in daily weight gain. Although protein gain percentage decreases during growth (Baker, 2009), the standard metabolic rate increases in adult birds as they age, (Briga & Verhulst, 2021), possibly implying the 12-month-old period is crucial for pigeons, as is their body maturation.

Age-associated variations in body weight and carcass traits significantly influence meat quality parameters, including pH, color, water-holding capacity, cooking loss, shear force, and texture (Mir et al., 2017; Wang et al., 2025). These quality traits are driven mainly by age-related changes in chemical composition and protein structure as the animal ages (Pearce et al., 2011). For example, inosine monophosphate levels in chicken breast reach their peak at 180 days, contributing to an increased umami flavor (Huang et al., 2024). Similarly, older ducks (900 days) show higher levels of amino acids such as aspartic acid and threonine compared with younger ducks (60 days) (Gu et al., 2025). Despite these insights, studies focusing on the nutritional and molecular characteristics of pigeon meat at different slaughter ages remain scarce, leaving a gap in the development of age-specific market strategies. Therefore, investigating age-related proteomic and metabolomic variations in pigeon meat is crucial for improving meat quality evaluation and informing optimal production decisions.

Metabolomics and proteomics have emerged as powerful post-genomic tools in meat science, providing new avenues for exploring the biochemical mechanisms underlying meat quality and processing.

* Corresponding author at: College of Animal Science and Technology, Yangzhou University, 225009 Yangzhou, PR China.
E-mail address: hmyang@yzu.edu.cn (H. Yang).
[1] These authors contributed equally to this work and should be considered co-first authors

https://doi.org/10.1016/j.fochx.2026.103839
Received 12 August 2025; Received in revised form 18 January 2026; Accepted 4 April 2026
Available online 15 April 2026

Untargeted metabolomics enables the comprehensive profiling of small molecules (molecular weight < 1500 Da) in meat, identifying metabolites that affect its quality attributes (Sidira, Smaoui and Varzakas, 2024). Meanwhile, data-independent acquisition (DIA)-based proteomics offers precise peptide quantification and enhanced protein identification. Chen et al. (2023) employed metabolomic techniques to investigate the dynamic metabolic changes that influence meat flavor formation in chickens at different growth stages. Similarly, integrated proteomic and metabolomic approaches have been utilized to identify candidate biomarkers distinguishing young and mature duck meat (Zhang et al., 2023).

However, integrated analyses combining proteomic and metabolomic data to explore age-dependent molecular variations in pigeon meat remain limited. To address this gap, the present study examined the breast muscle characteristics of 28-day-old (D28) and 12-month-old (M12) White King pigeons. DIA-based proteomic and untargeted metabolomic analyses were employed to identify differential protein expression and metabolite composition associated with age. Furthermore, integrative analysis was conducted to elucidate the molecular pathways underlying age-related differences in pigeon meat quality. These findings offer valuable insights into the biochemical mechanisms that govern meat quality across different ages, establishing a scientific foundation for developing age-based selection and processing strategies in pigeon production.

2. Materials and methods

2.1. Ethics approval

The study was approved by the Institutional Animal Care and Use Committee of the Department of Animal Science and Technology at Yangzhou University (Approval number SYXK [Su] 2016–0020, China). All procedures involving animals were conducted in strict accordance with the 2008 Standards for the Administration of Experimental Practices (Jiangsu, China).

2.2. Sample collection

Sixteen female White King pigeons were sourced from Donggao Pigeon Breeding Farm (Nanjing, China), comprising eight D28 and eight M12 birds. All pigeons were raised under identical conditions with *ad libitum* access to feed and water. Experimenters humanely euthanized birds by severing the jugular vein on one side of the neck under chloroform anesthesia inhalation to guarantee a rapid and painless death (following the "GB/T 19478–2018" standard). The right breast muscles were collected immediately and divided for omics analysis (selected five of the samples), texture profile analysis (TPA), and histological sectioning. The left breast muscles were used for physicochemical analyses.

2.3. Hematoxylin and eosin (HE) staining

Breast muscle tissues were fixed in 4% paraformaldehyde and sectioned into 5 μm slices. All sections were stained using the HE staining kit (Servicebio, Wuhan, China) and imaged under a light microscope (Olympus, Tokyo, Japan). For each sample, three representative areas comprising about 250 muscle fibers in total were selected. ImageJ software was used to calculate the fiber area ratio (%), fiber diameter (μm), and cross-sectional area of individual fibers (μm^2). In short, the field was first converted into an 8-bit grayscale image, and mapping to unified scales was done. Then, set the threshold in grayscale images and determine the corresponding value.

2.4. Meat quality measurement

2.4.1. pH measurement

The pH values were recorded at 1 h (pH_1) and 24 h (pH_{24}) post-muscle storage at 4 °C using a portable pH meter (DELTA 320, Mettler Toledo, Columbus, OH, USA). Measurements were taken at three locations on the same muscle sample. The instrument was calibrated before use with standard buffers at pH 4.0 and pH 7.0 using a two-point calibration method.

2.4.2. Meat color measurement

Meat color was assessed at 1 h and 24 h after slaughter using a colorimeter (Minolta CR400, Konica Minolta, Tokyo, Japan) based on the CIELAB system: L* (lightness), a* (redness), and b* (yellowness). The device was calibrated against a standard white calibration plate before use.

$$\Delta pH = pH_{24} - pH_1$$

2.4.3. Water-loss rate

To determine the water-loss rate, trimmed muscle samples were weighed (W_1) and then subjected to a 5-min pressing procedure using 16 layers of filter paper on both sides. After pressing, samples were reweighed (W_2). The water-loss rate of meat was determined by comparing its weight before and after the test. Water-loss rate (%) was calculated as:

$$\text{Water} - \text{loss rate} = (W_1 - W_2)/W_1 \times 100$$

2.4.4. Cooking loss calculation

Breast muscle samples were stored at 4 °C for 24 h, then weighed and sealed in individual sterile bags. The bags were then immersed in a water bath at 80 °C until the meat samples inside achieved an internal temperature of 70 °C. A thermometer was used to monitor the temperature of both the meat samples and the water bath. After cooling to room temperature, the cooked meat samples were dried with filter papers and reweighed, and the percentage of weight loss in the meat samples before and after cooking was calculated as the cooking loss.

2.4.5. Shear force measurement

After measuring the cooking loss, muscle samples were cut in a direction parallel to the muscle fibers into segments measuring 2.5 cm × 1 cm × 1 cm. Samples were cooled to 4 °C in a refrigerator and then subjected to shear force analysis.

2.4.6. TPA test

TPA was performed using a TMS-PRO texture analyzer (FTC, Sterling, USA) with a 2500 N load cell. Pigeon breast muscle samples (25 mm × 10 mm × 10 mm) underwent a double compression cycle under the following conditions: test speed, 20 mm/min; sample deformation, 20%; load cell height, 20 mm; trigger force, 30 N. TPA parameters (hardness, elasticity, cohesiveness, and chewiness) were calculated from force-time curves using FTC-PRO software (FTC, Sterling, USA). All measurements were conducted in triplicate.

2.5. Metabolome data processing

Sample pre-treatment, extraction, metabolite identification, and quantification were conducted at BGI-Shenzhen (Shenzhen, China) following established protocols. Untargeted metabolomic profiling was performed using ultra-high-performance liquid chromatography coupled with tandem mass spectrometry (UHPLC-MS/MS) on a Q Exactive HF high-resolution mass spectrometer (Thermo Fisher Scientific, USA). Data acquisition was conducted in both positive and negative ion modes to improve metabolite coverage. Variable Importance in Projection (VIP) scores were calculated for the first two principal

components derived from Orthogonal Partial Least Squares Discriminant Analysis (OPLS-DA). Differential metabolites were identified based on a combination of VIP scores, fold change (FC), and *q*-values obtained from univariate statistical analysis. For peptide preparation, samples were digested using trypsin at a 1:20 enzyme-to-protein mass ratio and incubated at 37 °C for 4 h. Following digestion, samples were centrifuged at 12,000 ×*g* for 15 min at 20 °C, and the supernatant was collected. A volume of 100 μL of 0.5 M TEAB was added to each ultrafiltration tube, followed by centrifugation at 12,000 ×*g* for 15 min at 20 °C. The digested peptide solution was then lyophilized. The dried peptides were resuspended in mobile phase A (0.1% formic acid in H_2O) and centrifuged at 20,000 ×*g* for 10 min. The resulting supernatant was used for injection. Separation was carried out using a Vanquish Neo UHPLC system (Thermo Fisher Scientific) equipped with an EASY-Spray™ HPLC column (150 μm × 15 cm, Thermo Fisher Scientific, USA). The nanoliter liquid phase separation was then directly introduced into the mass spectrometer for analysis.

2.6. Proteomics analysis

2.6.1. Protein extraction and quality control

Protein extraction was performed as previously described by Cui et al. (2022). The extracted proteins were subjected to quality control using Bradford assay and SDS-PAGE. A standard curve was generated using bovine serum albumin (BSA) at a concentration of 0.2 μg/μL. A series of standard proteins (0.2 μg/μL BSA) were added sequentially to the 96-well microtiter plates (A1 to A10), with volumes of 0, 2, 4, 6, 8, 10, 12, 14, 16, and 18 μL. Then, 20, 18, 16, 14, 12, 10, 8, 6, 4, and 2 μL of pure water were added to each well. Then, 180 μL of Coomassie Brilliant Blue G-250 working reagent was added to each well. The optical density (OD) at 595 nm was measured using a microplate reader, and a standard curve was constructed by plotting OD values against known protein concentrations. Sample protein solutions were diluted accordingly, and 20 μL of each diluted sample was mixed with 180 μL of the same dye reagent. The OD at 595 nm was measured, and the protein concentration was calculated based on the standard curve. For SDS-PAGE, 10 μg of each protein sample was mixed with loading buffer, heated at 95 °C for 5 min, and centrifuged at 25,000 ×*g* for 5 min. The supernatant was loaded onto a 12% SDS polyacrylamide gel. Electrophoresis was carried out at 120 V for 120 min. Gels were stained with Coomassie Brilliant Blue for 2 h, followed by decolorization using a solution of 40% ethanol and 10% acetic acid. The decolorization process was repeated 3–5 times, with each cycle lasting 30 min on a shaker.

2.6.2. Proteolysis

A total of 100 μg of protein from each sample was transferred to a 10-kDa ultrafiltration tube, and the volume was adjusted to 100 μL to ensure consistency across all samples. The samples were centrifuged at 12,000 ×*g* for 20 min at 20 °C to separate the protein solution. Then, 100 μL of 0.5 M TEAB was added, followed by centrifugation at 12,000 ×*g* for 20 min at 20 °C. This washing step was repeated three times. Afterward, the collection tube was replaced with a new one. Trypsin digestion was performed by adding enzyme at a trypsin-to-protein ratio of 1:20 and incubating the mixture at 37 °C for 4 h. After enzymatic digestion, the peptide solution was centrifuged at 120,000 ×*g* for 15 min at 20 °C, and the peptide-containing supernatant was collected. An additional 100 μL of 0.5 M TEAB was added to the ultrafiltration tube, followed by centrifugation at 12,000 ×*g* for 15 min at 20 °C. The final peptide fractions were then freeze-dried for further analysis.

2.6.3. DIA analysis by nano-LC-MS/MS

Lyophilized peptide samples were reconstituted in mobile phase A (0.1% formic acid in H_2O) and centrifuged at 20,000 ×*g* for 10 min. The supernatant was collected for injection. Peptide separation was performed on a Vanquish Neo UHPLC system (Thermo Fisher Scientific, USA) using an EASY-Spray™ HPLC column (150 μm × 15 cm, Thermo Fisher Scientific, USA) at a flow rate of 2.5 μL/min. The chromatographic gradient was as follows: 0–4 min, mobile phase B (80% acetonitrile, 0.1% formic acid) increased from 4% to 25%; 4–5 min, mobile phase B increased to 35%; 5.8–6.2 min, mobile phase B increased to 99% with the flow rate increased to 3 μL/min; 6.2–6.9 min, held at 99% mobile phase B. The nanoliter liquid phase separation was then directly connected to a Thermo Astral tandem mass spectrometer *via* a nano-ESI source for DIA analysis. The mass spectrometer was configured with an ion source voltage of 1.8 kV. The MS1 scan range was set from 380 to 980 *m/z* with a resolution of 240,000 and a maximum ion injection time (MIT) of 5 ms. The 380–980 *m/z* range was divided into 300 acquisition windows for continuous DIA fragmentation. Ion fragmentation was performed using higher-energy collisional dissociation (HCD) with a normalized collision energy (NCE) of 25. Fragment ions were detected in the astral region with a secondary resolution, and the MIT was set at 3 ms. Automatic gain control (AGC) targets were set to 500% for both MS1 and MS2 levels.

2.7. Statistical analysis

Data were expressed as mean ± SEM. Statistical comparisons were conducted using the independent samples *t*-test in SPSS v25.0 (IBM, Armonk, NY, USA). A P value <0.05 was considered statistically significant.

3. Results

3.1. Comparison of meat quality traits among ages

To evaluate meat quality across age groups, parameters including pH, meat color, water-holding capacity, cooking loss, shear force, and TPA were measured. Significant age-related effects were observed on the physical and chemical properties of muscle tissue (Table 1). Breast muscle color was affected by age, with D28 pigeons showing higher L*, a*, and b* values both immediately and at 24 h postmortem ($P < 0.05$). Cooking loss was greater in M12 pigeons than in D28 pigeons ($P < 0.05$), although no significant differences were seen within each group in water-loss rate ($P > 0.05$). Lower shear force and TPA parameters, including hardness, cohesiveness, and gumminess, were detected in D28 pigeons ($P < 0.05$). While no significant differences were observed between groups in pH measured at 1 h and 24 h postmortem ($P > 0.05$), a lower ΔpH was observed in younger pigeons ($P < 0.05$).

3.2. Comparison of muscle fiber morphology traits among ages

To facilitate the comparison of muscle fiber morphology, histological characteristics were examined and quantified (Fig. 1). Pigeon age had a significant effect on both fiber diameter and cross-sectional area (Fig. 1C). Breast muscle fibers in M12 pigeons displayed significantly larger diameter and size compared with those in D28 pigeons ($P < 0.01$ and $P < 0.05$, respectively).

3.3. Proteomic profiles of muscle components among ages

The principal component analysis (PCA) scatter plot showed distinct cluster formations for the two groups being compared, with clear separations observed between the samples (Fig. 2A). Pearson correlation analysis demonstrated high intra-group correlation and model stability ($R > 0.9$, Fig. 2B). DIA-based proteomic quantification identified 37,143 peptide sequences and 3168 proteins (Fig. 2C). Based on selection criteria of FC > 2 and $P < 0.05$ in each pairwise comparison, a total of 220 down-regulated and 18 up-regulated differentially expressed proteins (DEPs) were identified (Fig. 2D). The hierarchical clustering of 238 DEPs showed that most DEP expression patterns were significantly lower in 12-month-old pigeons than in 28-day-old pigeons (Fig. 2E).

Functional annotation of DEPs using Gene Ontology (GO)

Table 1
Comparison of muscle physical and chemical indicators contents among pigeon meat of different ages.

Items		Groups		*P* value
		28 day old	12 month old	
pH_1		5.4133 ± 0.00658[a]	5.38 ± 0.03909[a]	0.431
pH_{24}		5.4933 ± 0.01225[a]	5.4919 ± 0.03756[a]	0.976
ΔpH		0.078333 ± 0.011426[b]	0.111905 ± 0.007762[a]	0.033
Meat color	L*	39.0627 ± 0.85782 [A]	34.8981 ± 0.49735[B]	0.001
	a*	18.696 ± 0.20213 [A]	16.2771 ± 0.52855[B]	0.004
	b*	13.456 ± 0.66637 [A]	10.6081 ± 0.24022[B]	0.01
	L_{24}	40.8347 ± 0.60449 [A]	35.6867 ± 0.19724[B]	0.001
	a_{24}	19.404 ± 0.3302 [A]	16.7757 ± 0.23132[B]	<0.001
	b_{24}	16.152 ± 0.77551 [A]	10.6676 ± 0.18524[B]	0.002
Water-loss rate (%)		17.64 ± 0.00426[a]	17.04 ± 0.0108[a]	0.353
Cooking loss (%)		25.87 ± 0.00727[B]	28.96 ± 0.00566 [A]	0.007
Shear force (N)		4.033 ± 0.69984[B]	16.435 ± 1.06549 [A]	<0.001
Textural profile analysis (TPA)	hardness	72.0667 ± 1.6231[b]	95.8333 ± 6.3881[a]	0.023
	stringiness	102.6333 ± 5.98658[a]	111.35 ± 16.84207[a]	0.651
	cohesiveness	0.4133 ± 0.00667[b]	0.4567 ± 0.00882[a]	0.017
	springiness	0.4367 ± 0.0348[a]	0.52 ± 0.07371[a]	0.364
	gumminess	29.8333 ± 0.21858[b]	43.8 ± 3.1241[a]	0.011
	chewiness	13.0567 ± 1.07307[a]	23.17 ± 4.99057[a]	0.119

categorized them into biological processes (BP), cellular components (CC), and molecular functions (MF) (Fig. 3A). Among 238 DEPs, 38 were significantly enriched in BP terms related to metabolic processes, with 34 down-regulated and 4 up-regulated. KEGG pathway analysis showed enrichment primarily in metabolism-related pathways (Fig. 3B). Integration of expression data and enrichment results using a circular diagram facilitated dimensionality reduction and visualization of associations between metabolic terms and DEPs (Fig. 3C). A protein-protein interaction (PPI) network constructed using STRING revealed interactions among metabolism-associated DEPs (Fig. 3F). Pearson correlation analysis between meat quality phenotypes and key DEPs identified 20 positive and 29 negative correlations ($|R| > 0.5$, $P < 0.05$) (Fig. 3D). These analyses highlighted several proteins, including A306_00011918 (A0A2I0LN79, FC = 0.336), A306_00011919 (A0A2I0LN63, FC = 0.217), ENPP1 (A0A2I0M9P4, FC = 0.388), TKT (A0A2I0MEF2, FC = 0.494), and ALDH18A1 (A0A2I0MUI8, FC = 0.441), as contributors to eight distinct pathways associated with protein metabolism. These pathways included β-alanine metabolism, glycine, serine and threonine metabolism, phenylalanine metabolism, and others (Fig. 3E).

3.4. Metabolomic profiles of muscle components among ages

PCA and OPLS-DA were conducted based on the metabolites identified in pigeon breast muscle to differentiate the two groups of samples of different ages visually. The PCA score plot indicated effective quality control clustering, with the total variance explained by PCA1 and PCA2 at 25.91% and 11.7%, respectively (Fig. 4A). OPLS-DA further demonstrated a clear separation between age groups (Fig. 4B). To assess the quality of the model without overfitting risk, 200 response permutation tests were conducted on the OPLS-DA model. The prediction parameters R^2 and Q^2 of the OPLS-DA permutation tests are presented in Fig. 4C. Following data standardization, differentially expressed metabolites (DEMs) between the two groups were identified using volcano plots, based on the filtering criteria FC > 1.2 or < 0.83 and *q*-value <0.05 (Fig. 4D). A total of 238 differential metabolites were detected in the mix modes from the two groups, with 130 up-regulated and 108 down-regulated. The hierarchical clustering of these metabolites is presented as a heatmap (Fig. 4E), showing consistent color distributions among biological replicates within each group and distinct differences between the two age groups (M12 *vs.* D28). The classification of these common DEMs according to their chemical nature revealed that the top five most abundant superclass levels comprise lipids and lipid-like molecules (16.81%), organoheterocyclic compounds (14.29%), benzenoids (13.45%), organic acids and derivatives (12.18%), and phenylpropanoids and polyketides (9.24%) (Fig. 4F). KEGG pathway enrichment analysis demonstrated that these DEMs were mainly enriched in ABC transporters (map02010), biosynthesis of amino acids (map01230), D-amino acid metabolism (map00470), arginine and proline metabolism (map00330), and arginine biosynthesis (map00220) (Fig. 4G). Furthermore, key metabolites identified included L-histidine (FC = 0.216), L-arginine (FC = 0.560), 4-hydroxyproline (FC = 0.149), D-sedoheptulose 7-phosphate (FC = 0.465), and L-glutamic acid 5-phosphate (FC = 0.120), each participating in pathways associated with nutrient metabolism (Fig. 4H).

3.5. Co-analysis of proteomics and metabolomics data

To investigate age-related differences in muscle composition, PCA was conducted on both proteomic and metabolomic datasets, separately and in combination (Fig. 5A). Integration of both omics datasets resulted in improved clustering and more pronounced inter-group differences. The heatmap displayed a strong correlation between differential metabolites and proteins (Fig. 5B), which was consistent with the PCA results and confirmed the robustness of the combined analysis. A Venn diagram revealed that 13 KEGG pathways were shared between the proteomic and metabolomic analyses (Fig. 5C). To further assess age-related effects on meat quality, the top 10 enriched KEGG pathways were analyzed, six of which were involved in amino acid metabolism. These included β-alanine metabolism, arginine and proline metabolism, cysteine and methionine metabolism, glycine, serine and threonine metabolism, histidine metabolism, and biosynthesis of amino acids (Fig. 5D and Fig. 5E).

Detailed analysis of pathways associated with protein metabolism is presented in Fig. 6. At the proteomic level, age affected the amino acid biosynthesis pathway *via* ALDH18A1, GATM, A306_00011918, and A306_00011919. These proteins also influenced the pentose phosphate pathway and purine metabolism through TKT, ENPP1, and A306_00000303, facilitating cyclic metabolic flow. At the metabolomic level, aging was associated with reduced expression of L-glutamyl 5-phosphate, sedoheptulose-7-phosphate, imidazole-acetol-phosphate, 4-hydroxyproline, L-histidine, L-arginine, and guanosine, which in turn affected amino acid biosynthesis and energy metabolism. These findings demonstrate that aging affects meat quality through complex and interconnected effects on proteins, metabolites, and metabolic pathways related to amino acid biosynthesis.

4. Discussion

Pigeon meat has gained recognition as a nutritious and high-quality protein source, contributing to the steady growth of the pigeon industry. In China, pigeon ranks as the fourth most widely consumed poultry product after chicken, duck, and goose (Ji et al., 2022). Understanding the influence of animal age on meat quality is critical for optimizing

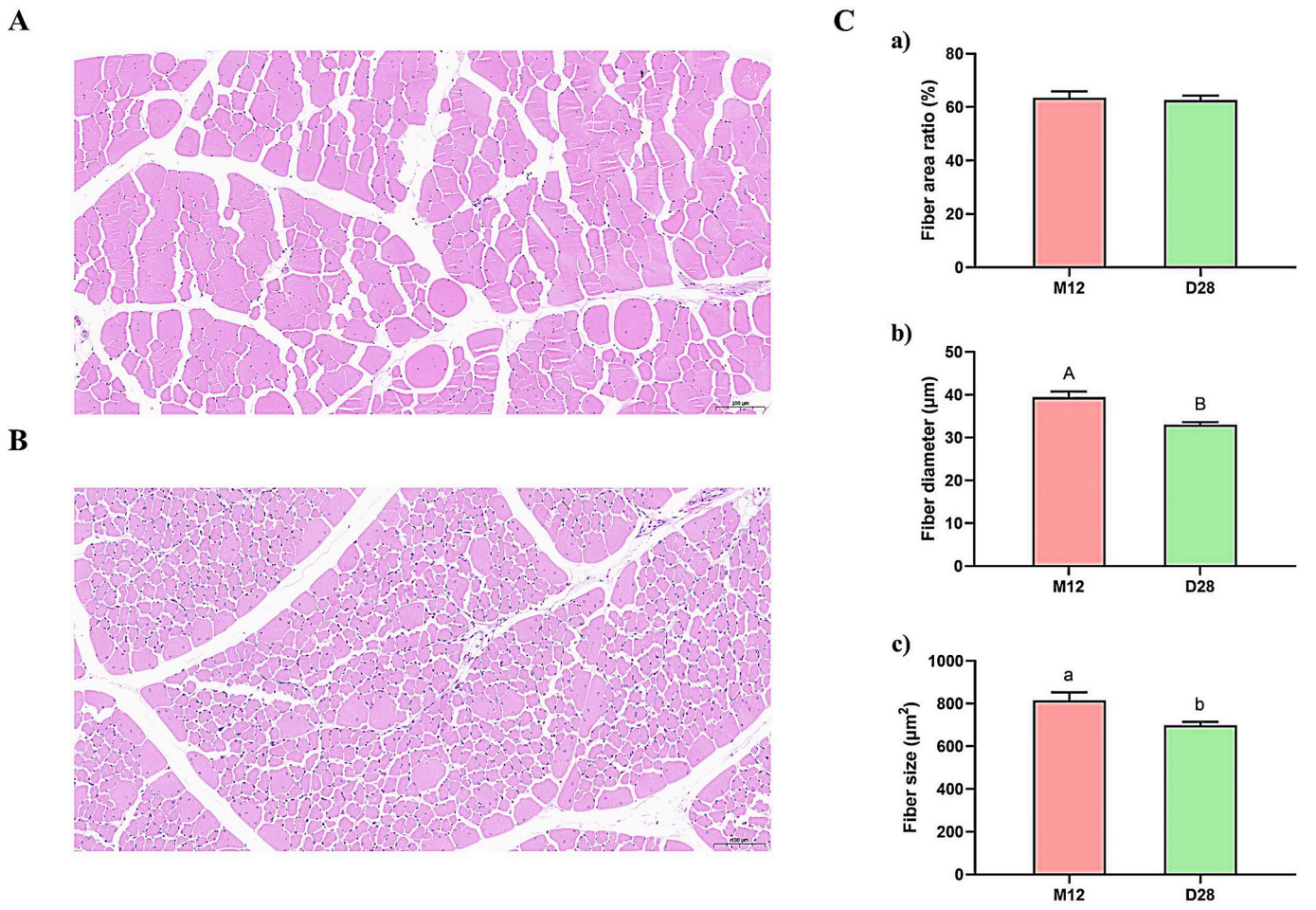

Fig. 1. Histological comparison of muscle fibers and bundles in pigeons of different ages. (A) Hematoxylin and eosin (H&E) staining of muscle tissue from 12-month-old pigeons. Scale bar = 100 μm. (B) H&E staining of muscle tissue from 28-day-old pigeons. Scale bar = 100 μm. (C) Quantitative comparison of histological characteristics between the two age groups: (a) muscle fiber area ratio; (b) muscle fiber diameter; (c) muscle fiber size.

production and marketing strategies (Chen et al., 2024a). A comparative analysis was conducted to assess the quality of meat from pigeons of differing ages (M12 and D28). The color of fresh meat is among the most crucial features at the time of purchase (King et al., 2023). In this study, breast meat from 28-day-old pigeons displayed more redness (a* and a_{24} values) compared with that from 12-month-old pigeons. These observations are consistent with the findings of Rajčić et al. (2024), who reported a decline in meat redness in broiler breasts from 42 to 70 days of age. With advancing age, myofibers enlarge, and peripheral capillary density decreases due to marginalization (Velleman, 2015), resulting in reduced meat redness. Furthermore, younger pigeon meat displayed greater L*, a*, and b* values, which aligns with results reported by Popova et al. (2023), who observed that the meat color of 5-week-old chickens breast was lighter than that of older birds.

The results further indicated that pH values of M12 and D28 pigeon meat were not significantly different, consistent with previous findings in duck and goose meat (Gu et al., 2024; Weng et al., 2021). Water-holding capacity, a key trait affected by partial protein denaturation under postmortem acidic conditions, was also assessed (Petracci et al., 2015). No significant difference in water-loss rate was seen between the two age groups; however, the cooking loss in younger pigeons was significantly lower ($P < 0.05$). The differing trends observed in drip loss and cooking loss suggest variations in water-holding capacity between raw and cooked meat (Li et al., 2019). Li (2006) concluded that gumminess reflects both hardness and cohesiveness in hens. In this study, hardness, cohesiveness, and gumminess were all significantly higher in older pigeons. Shear force values for breast meat were found to be age-dependent, with higher values recorded in M12 birds. This finding agrees with those of Park and Kim (2021), who reported increased shear force in chicken breast meat from 28 to 34 days of age. Previous studies have associated increased muscle fiber size with elevated shear force and increased toughness (Guan et al., 2013). In this study, larger fiber diameter and size were observed in the breast meat of M12 pigeons, supporting this pattern. Zhao et al. (2024) found fiber density in goose muscle decreased with advancing age, while fiber diameter and area showed the opposite trend. It may be the reason why fiber diameter and size continued increasing, but the area ratio still remained stable in our study.

Metabolomics has been employed in foodomics to identify molecular features of food and examine its compound composition (Valdés et al., 2022). In this study, metabolic differences between M12 and D28 pigeon breast muscles were evaluated to determine the metabolic profiles of each age group. The majority of DEMs identified through KEGG pathway analysis were downregulated in the M12 group compared with D28. Lipid metabolism accounts for the largest proportion, of which the most diverse lipid type was glycerophospholipid (Wang et al., 2023a). In the M12 *versus* D28 comparison, downregulated lipids contained LysoPE (20:3(11Z,14Z,17Z)/0:0), LysoPC(16:1(9Z)/0:0), PC(14:0/20:4), PC (16:0/20:3), PC(18:0/20:2), and PC(18:0/22:4). One study revealed that most differential PC and PE metabolites were downregulated with intramuscular fat content increase (Chen et al., 2025). Besides, changes in glycerides, including TG and DG content, that are closely associated with the growth process of pigeons, gradually increased with age, aligning with Chen et al., (2024b). The intramuscular fat content of

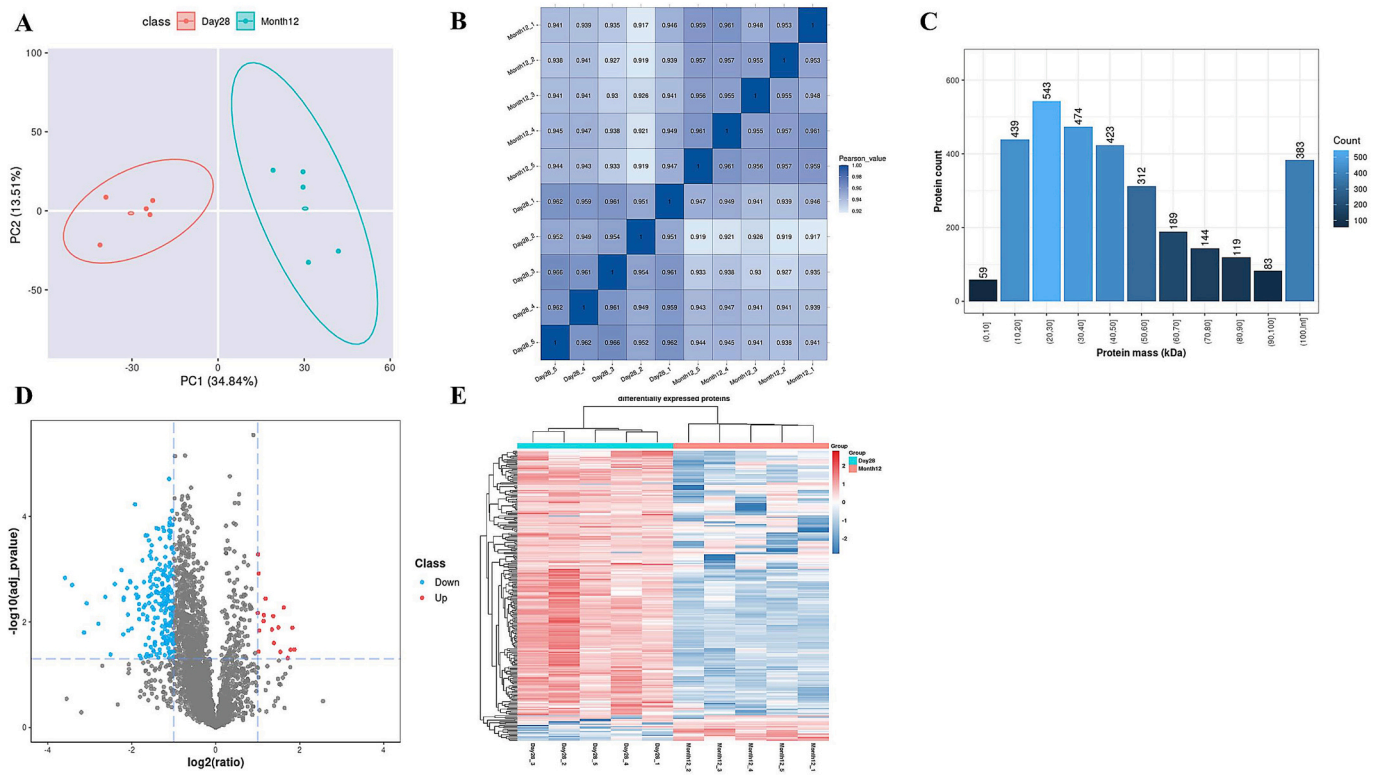

Fig. 2. Multivariate statistical analysis of pigeon muscle proteomics across ages. (A) Principal component analysis (PCA) scores showing the separation of the two groups. (B) Correlation analysis between the two age groups. (C) Bar chart illustrating the distribution of protein quality. (D) Volcano plot showing significantly differentially abundant proteins. (E) Heatmap of differentially expressed proteins between the two groups.

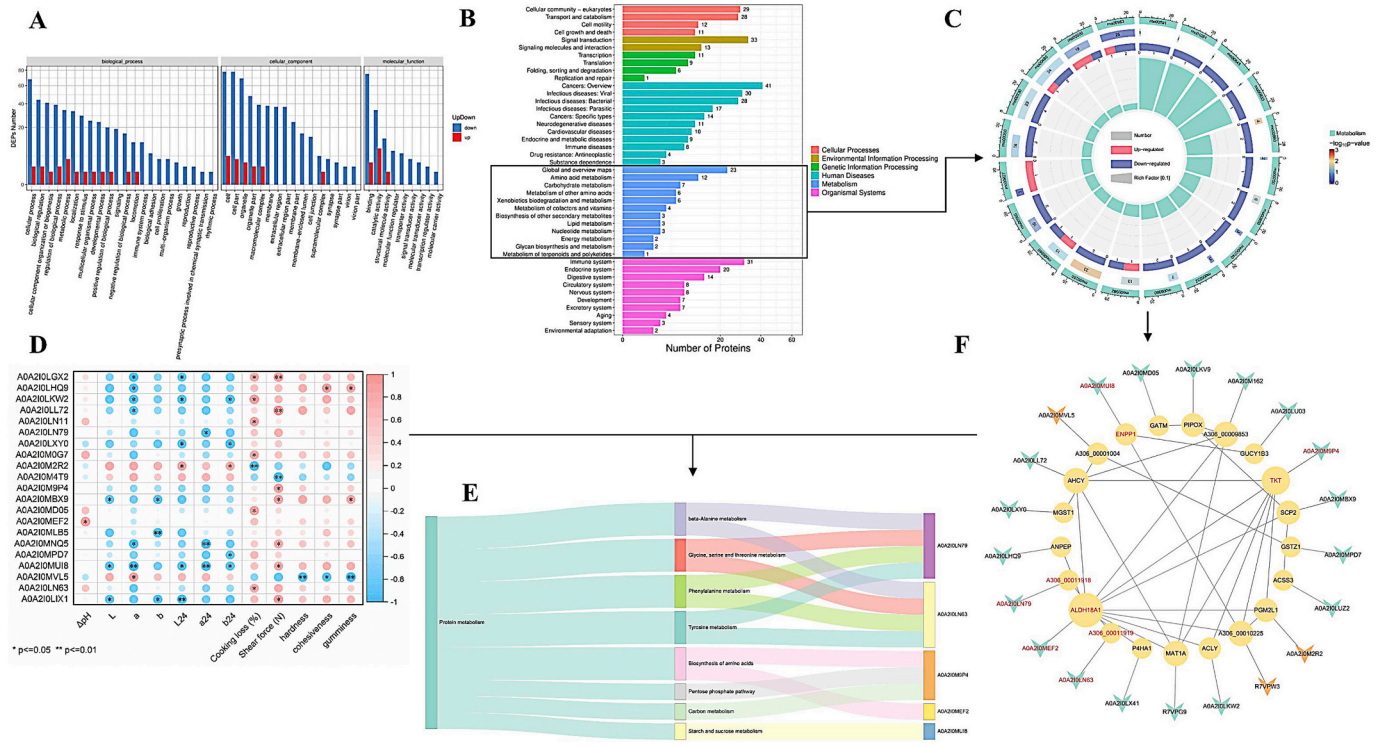

Fig. 3. Functional analysis of differentially abundant proteins. (A) Gene Ontology (GO) enrichment analysis of differentially expressed proteins. (B) KEGG pathway classification and annotation. (C) KEGG enrichment analysis highlighting metabolic pathways. (D) Correlation analysis between differentially abundant proteins and phenotypic parameters. (E) Sankey diagram of KEGG pathways related to protein metabolism. (F) Protein-protein interaction (PPI) network analysis of candidate proteins.

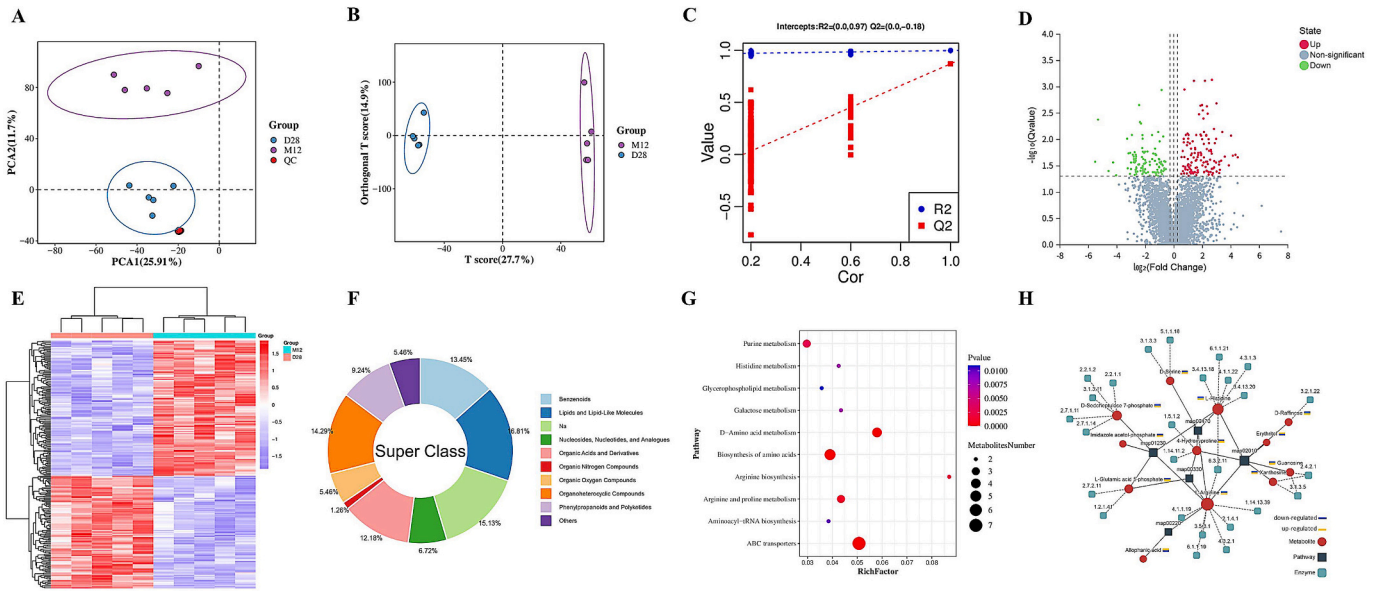

Fig. 4. Overview of metabolomics profiling in pigeon meat across the two age groups. (A, B) PCA and OPLS-DA score plots demonstrating the separation of the two groups. (C) Permutation test results for the OPLS-DA model (200 repetitions). (D) Volcano plot showing differentially abundant metabolites. (E) Heatmap of differential metabolites. (F) Classification of differential metabolites at the superclass level. (G) KEGG-based pathway prediction of differential metabolites. (H) Enrichment network diagram of pathways involving differential metabolites.

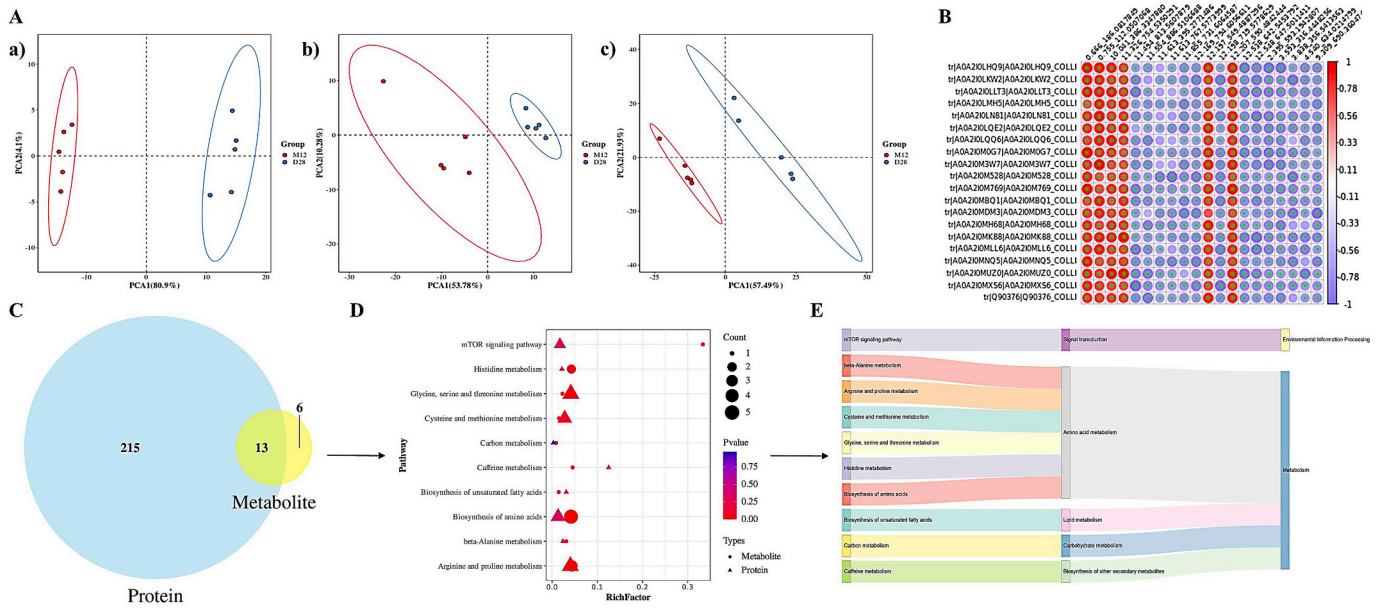

Fig. 5. Integrated analysis of shared functional signaling pathways between proteome and metabolome. (A) PCA score plots illustrating group separation across datasets: (a) metabolomics; (b) proteomics; (c) combined metabolomics and proteomics. (B) Correlation heatmap between metabolomic and proteomic datasets. (C) Venn diagram of shared KEGG pathways. (D) Bubble plots of KEGG pathway enrichment based on both datasets. (E) Sankey diagram illustrating shared KEGG pathways involved in metabolic regulation.

older poultry was significantly higher than that of younger ones (Yuan et al., 2022), indicating a notable fluctuation in these lipid metabolites with age. The levels of amino acids and their derivatives—L-histidine, L-arginine, and 4-hydroxyproline—were lower in M12 pigeons than in D28 birds. Deng et al. (2022) reported comparable findings in chickens between 60 and 75 days of age. A higher histidine content has been shown to slow the postmortem pH decline in fish muscle (Zeng et al., 2025), supporting our findings. Arginine has been previously associated with improved meat characteristics in broilers, resulting in increased L* value and reduced shear force (Jiao, Guo, Yang and Long, 2010). Similarly, Dou et al. (2023) reported that arginine enhances lamb meat quality by decreasing shear force and cooking loss; these findings align with our results. Hydroxyproline, a unique amino acid in collagen, could assess collagen quantity, and intramuscular collagen becomes less soluble as animals age (Markowsky et al., 2025). Dominik et al., (2011) demonstrated that higher collagen solubility contributes to more tender meat and lower maximum TPA force, consistent with the present study. Nucleotides are known to affect meat quality, particularly in terms of flavor (Poompramun et al., 2021). Levels of nucleotides and their metabolites, including guanosine and xanthosine, declined with age. These compounds contribute to purine metabolism, and the observed changes may reflect differences in physical activity between age groups (Wang

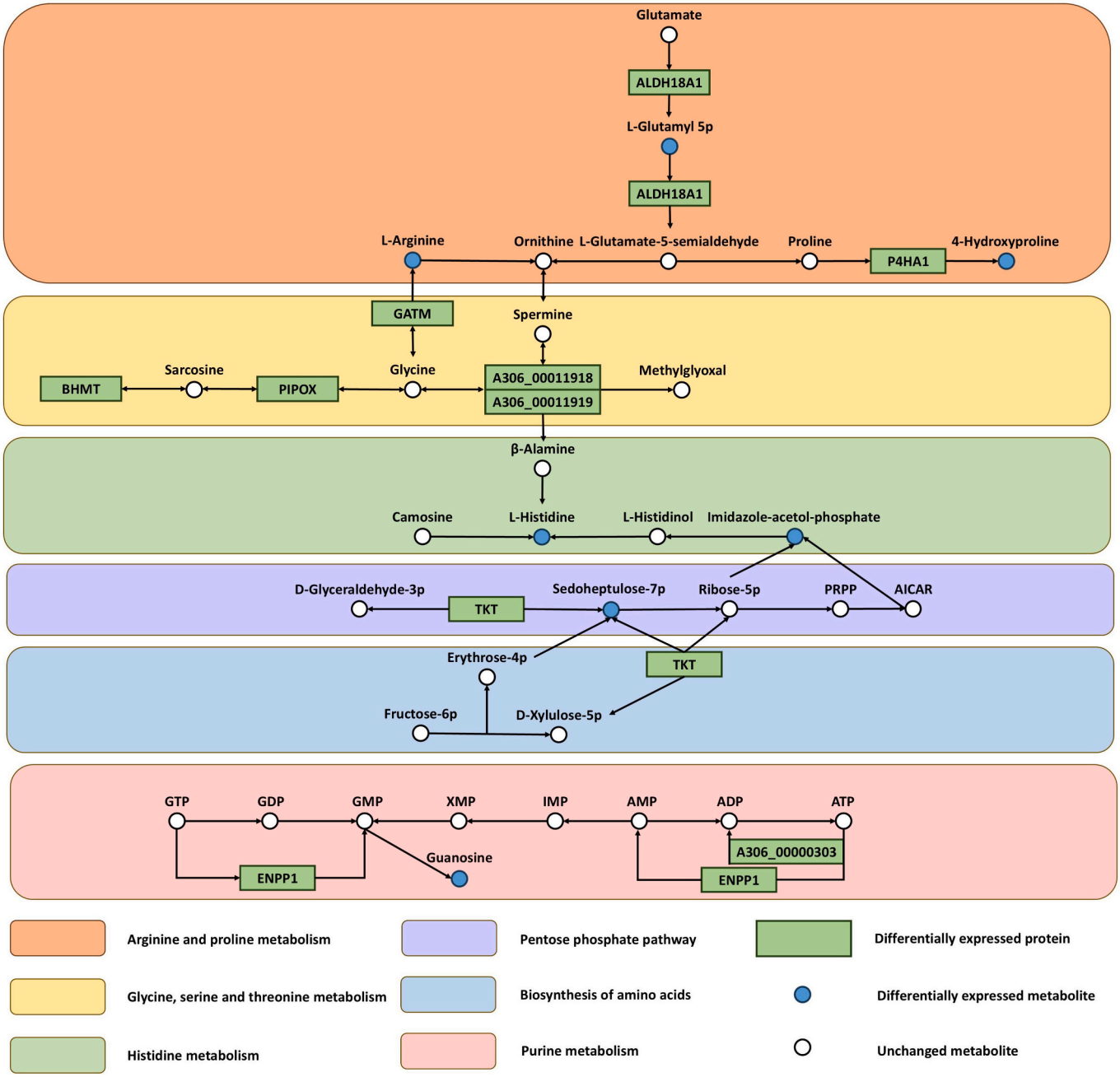

Fig. 6. Expression profiles of DEGs or DEPs from amino acid biosynthesis metabolism in pigeon meat of the two groups.

et al., 2024). Xanthosine levels were significantly higher in adult geese, potentially reflecting the effects of breed or sex (Wang et al., 2023b).

Proteomic methods in the field of meat science help examine the processes related to traits of meat quality (Cao et al., 2022). Insights into the biochemical processes affecting meat quality development are gained through advanced techniques in meat proteome analysis. In this study, the differences in protein composition between age groups were pronounced. A total of 238 DEPs were identified, among which candidate proteins—A306_00011918, A306_00011919, ENPP1, TKT, and ALDH18A1—may affect metabolites such as L-histidine, L-arginine, guanosine, D-sedoheptulose 7-phosphate, 4-hydroxyproline, and L-glutamic acid 5-phosphate through amino acid biosynthesis-related metabolic pathways. TKT is a protein involved in carbohydrate metabolism and is identified as being differentially deficient with age. TKT has been demonstrated to be intimately associated with glycolysis through the pentose phosphate pathway, a branch of glycolysis (Dang et al., 2022). Several proteomic studies have indicated a positive correlation between increased expression of proteins associated with glycolysis and meat tenderness (López-Pedrouso et al., 2021; Silva et al., 2019), which is consistent with our findings. ENPP1 regulates skeletal and soft tissue mineralization by generating inorganic pyrophosphate (Wu et al., 2025). In this study, ENNP1 was decreased in the M12 pigeon breast and positively correlated with shear force, supporting its role in meat texture. Similarly, in hybrid pigs, ENPP1 has been associated with increased inosine monophosphate deposition, which contributes to greater tenderness and flavor (Long et al., 2025), which could explain the reason for the tenderness and ENPP1 maintaining a falling trend with age. The loss of function of ALDH18A1 was found to be associated with larger lipid droplets and positively correlated with leanness in chickens (Tang et al., 2023). The intramuscular fat content is known to influence the visual assessment of meat color (Beličovska et al., 2024). Our experimental results demonstrated a negative correlation between

ALDH18A1 and meat color, suggesting that ALDH18A1 affects meat color by affecting fat deposition with age.

Utilizing both metabolomic and proteomic datasets together offers a promising means to understand the crucial pathways and molecular mechanisms that determine pigeon meat quality. The integrative analysis revealed significant regulation of amino acid biosynthesis between the two age groups. Both DEPs and DEMs were involved in amino acid metabolism pathways, including arginine and proline metabolism, glycine, serine, and threonine metabolism, histidine metabolism, the pentose phosphate pathway, and purine metabolism, either directly or indirectly. The combined analysis facilitated the identification of key DEPs and DEMs whose downregulation contributes significantly to the compositional differences in pigeon meat at different ages. These proteins and metabolites play key roles in the age-dependent quality characteristics of pigeon meat. These findings will facilitate the identification of molecular markers and metabolites that distinguish meat quality across ages.

5. Conclusion

The results showed that the D28 group exhibited higher L*, a*, and b* values, as well as lower ΔpH, shear force, cooking loss, hardness, cohesiveness, and gumminess. Metabolomic analysis identified amino acid biosynthesis as a key pathway, with declines in associated DEMs, including L-histidine, L-arginine, 4-hydroxyproline, D-sedoheptulose 7-phosphate, and L-glutamic acid 5-phosphate, exerting a significant effect. There were five key DEPs, A306_00011918, A306_00011919, ENPP1, TKT, and ALDH18A1, downregulated and closely linked to meat traits, indicating that substantial biochemical changes occur in pigeon meat with it ages. The study presents important evidence of metabolites and proteins controlling meat quality, shedding light on the processes involved in producing superior pigeon meat products. Furthermore, the findings reveal clear distinctions in meat characteristics across age groups, which may inform targeted marketing and optimal slaughter strategies.

CRediT authorship contribution statement

Ying Wang: Writing – review & editing, Supervision, Resources, Methodology, Conceptualization. **Dongzhi Miao:** Writing – original draft, Validation, Methodology, Investigation. **Jing Chen:** Validation, Methodology. **Haodong Zhang:** Validation, Methodology. **Wanqing Li:** Validation, Methodology. **Haiming Yang:** Conceptualization. **Zhiyue Wang:** Funding acquisition, Conceptualization.

Declaration of competing interest

The authors declare that they have no known competing financial interests or personal relationships that could have appeared to influence the work reported in this paper.

Acknowledgements

This study was funded by the the Postgraduate Research & Practice Innovation Program of Jiangsu Province [KYCX24_3811], the National Natural Science Foundation of China (32372875), and the Priority Academic Program Development of Jiangsu Higher Education Institutions (PAPD).

Appendix A. Supplementary data

Supplementary data to this article can be found online at https://doi.org/10.1016/j.fochx.2026.103839.

Data availability

Data will be made available on request.

References

Baker, D. H. (2009). Advances in protein-amino acid nutrition of poultry. *Amino Acids, 37*(1), 29–41.

Beličovska, D., Nikolova, A. S., & Petrov, P. (2024). Influence and role of fat on the sensory characteristics of meat products. *Macedonian Journal of Animal Science, 13*, 35–39.

Briga, M., & Verhulst, S. (2021). Mosaic metabolic ageing: Basal and standard metabolic rates age in opposite directions and independent of environmental quality, sex and life span in a passerine. *Functional Ecology, 35*(5), 1055–1068.

Cao, C., Xiao, Z., Ge, C., & Wu, Y. (2022). Application and research progress of proteomics in chicken meat quality and identification: A review. *Food Reviews International, 38*(3), 313–334.

Chang, L., Tang, Q., Zhang, R., Fu, S., Mu, C., Shen, X., & Bu, Z. (2023). Evaluation of meat quality of local pigeon varieties in China. *Animals (Basel), 13*(8), 1291.

Chen, G., Ling, X. Y., Xie, M. S., Xiong, Y. F., Li, T. T., Wang, Y., Shui, C. L., Li, C. M., Xu, B. C., & Ma, F. (2024a). Systematic evaluation of the meat qualities of free-range chicken (Xuan-Zhou) under different ages explored the optimal slaughter age. *Poultry Science, 103*(9), Article 104019.

Chen, L., Zhang, M., Feng, T., Liu, H., Lin, Y., & Bai, B. (2024b). Comparative characterization of flavor precursors and volatiles in chongming white goat of different ages by UPLC-MS/MS and GC-MS. *Food Chemistry: X, 24*, Article 101929.

Chen, X., Cao, J., Chang, C., Geng, A., Wang, H., Chu, Q., … Zhang, J. (2023). Effects of age on compounds, metabolites and meat quality in Beijing-you chicken breast meat. *Animals (Basel), 13*(21), 3419.

Chen, Z., Chen, Q., Zhang, W., Sun, Q., Liu, G., Wang, Y., … Zhang, J. (2025). Combined untargeted LC−MS metabolomics and lipidome reveal the key metabolites and genes of meat quality regulation and their regulatory mechanisms in chinese pigs. *ACS Food Science & Technology, 5*(12), 4578–4590.

Cui, Z., Ning, Z., Deng, X., Du, X., Amevor, F. K., Liu, L., … Zhao, X. (2022). Integrated proteomic and metabolomic analyses of chicken ovary revealed the crucial role of lipoprotein lipase on lipid metabolism and steroidogenesis during sexual maturity. *Frontiers in Physiology, 13*, Article 885030.

Dang, D. S., Zhai, C., Nair, M. N., Thornton, K. J., Sawalhah, M. N., & Matarneh, S. K. (2022). Tandem mass tag labeling to assess proteome differences between intermediate and very tender beef steaks. *Journal of Animal Science, 100*(8), skac042.

Deng, S., Xing, T., Li, C., Xu, X., & Zhou, G. (2022). The effect of breed and age on the growth performance, carcass traits and metabolic profile in breast muscle of chinese indigenous chickens. *Foods, 11*(3), 483.

Dominik, P., Pavlík, Z., Steinhauserová, I., Saláková, A., Buchtová, H., & Steinhauser, L. (2011). The effect of soluble collagen on the texture of fallow deer meat. *Maso International Brno, 1*, 57–61.

Dou, L., Sun, L., Liu, C., Su, L., Chen, X., Yang, Z., Hu, G., Zhang, M., Zhao, L., & Jin, Y. (2023). Effect of dietary arginine supplementation on protein synthesis, meat quality and flavor in growing lambs. *Meat Science, 204*, Article 109291.

Gao, C. Q., Yang, J. X., Chen, M. X., Yan, H. C., & Wang, X. Q. (2016). Growth curves and age-related changes in carcass characteristics, organs, serum parameters, and intestinal transporter gene expression in domestic pigeon (columba livia). *Poultry Science, 95*(4), 867–877.

Gu, T., Duan, M., Chen, L., Tian, Y., Xu, W., Zeng, T., & Lu, L. (2024). Proteomic-metabolomic combination analysis reveals novel biomarkers of meat quality that differ between young and older ducks. *Poultry Science, 103*(4), Article 103530.

Gu, T., Duan, M., Chen, L., Tian, Y., Xu, W., Zeng, T., & Lu, L. (2025). The difference between young and older ducks: Amino acid, free fatty acid, nucleotide compositions and breast muscle proteome. *Food Chemistry: X, 25*, Article 102117.

Guan, R. F., Lyu, F., Chen, X. Q., Ma, J. Q., Jiang, H., & Xiao, C. G. (2013). Meat quality traits of four chinese indigenous chicken breeds and one commercial broiler stock. *Journal of Zhejiang University-SCIENCE B, 14*(10), 896–902.

Huang, Y., Xu, C., Huang, X., Tan, Y., Li, S., & Yin, Z. (2024). Metabolome and transcriptome profiling reveals age-associated variations in meat quality and molecular mechanisms of taihe black-bone silky fowls. *Journal of Agricultural and Food Chemistry, 72*(39), 21946–21956.

Ji, F., Zhang, S., An, Y., Wang, Z., Shao, Y., Du, S., … Sun, X. (2022). Influence of dietary phosphorus concentrations on the performance of rearing pigeons (columba livia), and bone properties of squabs. *Poultry Science, 101*(4), Article 101744.

Jiang, H., Li, Y., Li, L., Chen, W., Zeng, X., Bai, W., & Xiao, G. (2022). Effects of different breeds and ages of meat pigeons on quality and flavor of pigeon soup. *Journal of Food Processing and Preservation, 46*(10), Article e16923.

Jiao, P., Guo, Y., Yang, X., & Long, F. (2010). Effects of dietary arginine and methionine levels on broiler carcass traits and meat quality. *Journal of Animal and Veterinary Advances, 9*(11), 1546–1551.

King, D. A., Hunt, M. C., Barbut, S., Claus, J. R., Cornforth, D. P., Joseph, P., & Weber, M. (2023). American meat science association guidelines for meat color measurement. *Meat and Muscle Biology, 6*(4).

Li, C. T. (2006). Myofibrillar protein extracts from spent hen meat to improve whole muscle processed meats. *Meat Science, 72*(3), 581–583.

Li, J., Yang, C., Peng, H., Yin, H., Wang, Y., Hu, Y., … Liu, Y. (2019). Effects of slaughter age on muscle characteristics and meat quality traits of Da-Heng meat type birds. *Animals (Basel), 10*(1), 69.

Long, Y., Zhang, N., Bi, Y., Ma, T., Paengkoum, P., Xiao, W., … Han, Y. (2025). Integrated transcriptomic analysis unveils molecular mechanisms regulating meat quality in newly improved black goat breeds. *npj Science of Food, 9*(1), 129.

López-Pedrouso, M., Lorenzo, J. M., Di Stasio, L., Brugiapaglia, A., & Franco, D. (2021). Quantitative proteomic analysis of beef tenderness of piemontese young bulls by SWATH-MS. *Food Chemistry, 356*, Article 129711.

Markowsky, M., Valente, T. S., Li, C., Roy, B. C., Juarez, M., & Bruce, H. L. (2025). Genetic architecture of collagen characteristics in beef. *Canadian Journal of Animal Science, 105*, 1–16.

Mir, N. A., Rafiq, A., Kumar, F., Singh, V., & Shukla, V. (2017). Determinants of broiler chicken meat quality and factors affecting them: A review. *Journal of Food Science and Technology, 54*(10), 2997–3009.

Park, S. Y., & Kim, H. Y. (2021). Effects of marketing ages on the physicochemical properties and sensory aspects of cured broiler chicken breast meat. *Foods, 10*(9), 2152.

Pearce, K. L., Rosenvold, K., Andersen, H. J., & Hopkins, D. L. (2011). Water distribution and mobility in meat during the conversion of muscle to meat and ageing and the impacts on fresh meat quality attributes-a review. *Meat Science, 89*(2), 111–124.

Petracci, M., Mudalal, S., Soglia, F., & Cavani, C. (2015). Meat quality in fast-growing broiler chickens. *World's Poultry Science Journal, 71*(2), 363–374.

Poompramun, C., Molee, W., Thumanu, K., & Molee, A. (2021). The significant influence of residual feed intake on flavor precursors and biomolecules in slow-growing Korat chicken meat. *Animal Bioscience, 34*, 1684–1694.

Popova, T., Petkov, E., Ignatova, M., Vlahova-Vangelova, D., Balev, D., Dragoev, S., … Dimov, K. (2023). Meat quality of male layer-type chickens slaughtered at different ages. *Agriculture, 13*(3), 624.

Rajčić, A., Bošković Cabrol, M., Glišić, M., Čobanović, N., Tomović, V., Laudanović, M., & Nešić, S. (2024). Pathomorphological and meat quality alterations connected with wooden breast in broiler chickens of different genotypes and slaughter ages. *Acta Veterinaria, 74*(2), 183–209.

Sidira, M., Smaoui, S., & Varzakas, T. (2024). Recent proteomics, metabolomics and lipidomics approaches in meat safety, Processing and Quality Analysis. *Applied Sciences, 14*(12), Article 5147.

Silva, L., Rodrigues, R., Assis, D., Benedeti, P., Duarte, M. S., & Chizzotti, M. L. (2019). Explaining meat quality of bulls and steers by differential proteome and phosphoproteome analysis of skeletal muscle. *Journal of Proteomics, 199*, 51–66.

Tang, Y., Yin, L., Liu, L., Chen, Q., Lin, Z., Zhang, D., … Liu, Y. (2023). Comparative analysis of different proteins and metabolites in the liver and ovary of local breeds of chicken and commercial chickens in the later laying period. *International Journal of Molecular Sciences, 24*(18), 14394.

Valdés, A., Álvarez-Rivera, G., Socas-Rodríguez, B., Herrero, M., Ibáñez, E., & Cifuentes, A. (2022). Foodomics: Analytical opportunities and challenges. *Analytical Chemistry, 94*(1), 366–381.

Velleman, S. G. (2015). Relationship of skeletal muscle development and growth to breast muscle myopathies: A review. *Avian Diseases, 59*(4), 525–531.

Wang, D., Qin, P., Zhang, K., Wang, Y., Guo, Y., Cheng, Z., … Liu, X. (2023a). Integrated LC/MS-based lipidomics and transcriptomics analyses revealed lipid composition heterogeneity between pectoralis intramuscular fat and abdominal fat and its regulatory mechanism in chicken. *Food Research International (Ottawa, Ont.), 172*, Article 113083.

Wang, L., Chen, X., Yang, Y., Ye, S., Gong, P., Wang, Y., … Qian, Y. (2025). The effect of duck breeds on carcass composition and meat quality at different slaughter ages. *Animals (Basel), 15*(14).

Wang, L., Gao, J., Li, G., Cheng, J., Yuan, G., Zhang, T., … Lu, H. (2024). Identification of metabolites in muscles of lueyang black-bone chickens: A comparative analysis of caged and cage-free rearing modes using untargeted metabolomic techniques. *Animals (Basel), 14*(14), 2041.

Wang, Y., Li, W., Zhang, C., Li, F., Yang, H., & Wang, Z. (2023b). Metabolomic comparison of meat quality and metabolites of geese breast muscle at different ages. *Food Chemistry: X, 19*, Article 100775.

Weng, K., Huo, W., Gu, T., Bao, Q., Hou, L. E., Zhang, Y., Zhang, Y., Xu, Q., & Chen, G. (2021). Effects of marketable ages on meat quality through fiber characteristics in the goose. *Poultry Science, 100*(2), 728–737.

Wu, G., Yu, M., Liu, T., Zhang, D., Chang, Y., Liu, Z., … Xu, C. (2025). Integration of multiomics data reveals selection characteristics of ITGB1 that are associated with size differentiation in pigs. *International Journal of Molecular Sciences, 26*(4), 1569.

Yang, P., Song, X., Wu, W., Zhang, L., Han, Z., Wang, X., … Zhang, Z. (2025). Nutritional profiling of breast muscle: A comparative study between yuzhong pigeons and european meat pigeons. *Food Chemistry: X, 25*, Article 102157.

Yuan, C., Jiang, Y., Wang, Z., Chen, G., Bai, H., & Chang, G. (2022). Indigenous, yellow-feathered chickens body measurements, carcass traits, and meat quality depending on marketable age. *Animals, 12*(18), 2422.

Zeng, X., Zhou, X. Q., Jiang, W. D., Wu, P., Liu, Y., Ma, Y. B., … Feng, L. (2025). Histidine improves flesh quality: An assessment of grass carp (ctenopharyngodon idella) muscle in terms of texture, nutritional value and flavor. *Food Chemistry, 474*, Article 143214.

Zhang, J., Chen, X., Cao, J., Chang, C., Geng, A., Wang, H., … Liu, H. (2023). Proteomic profiling of thigh meat at different ages of chicken for meat quality and development. *Foods, 12*(15), 2901.

Zhao, X., Cao, Y., Li, H., Wu, Y., Yao, Y., Wang, L., … Yao, Y. (2024). Development of myofibers and muscle transcriptomic analysis in growing yili geese. *Poultry Science, 103*(2), Article 103328.